WPJET4-CPR(18) 19985

P Dumortier et al.

Review of the JET ILA Scattering-Matrix Arc Detection System

Preprint of Paper to be submitted for publication in Proceeding of
30th Symposium on Fusion Technology (SOFT)

This work has been carried out within the framework of the EUROfusion Consortium and has received funding from the Euratom research and training programme 2014-2018 under grant agreement No 633053. The views and opinions expressed herein do not necessarily reflect those of the European Commission.

Review of the JET ILA Scattering-Matrix Arc Detection System

P. Dumortier[1,2], E. Lerche[1,2], F. Durodié[1], T. Blackman[2], W. Helou[3], I. Monakhov[2], C. Noble[2] and JET contributors*

EUROfusion Consortium, JET, Culham Science Centre, Abingdon, OX14 3DB, UK

[1]*LPP-ERM/KMS, TEC partner, Brussels, Belgium*
[2]*CCFE, Culham Science Centre, Abingdon, United Kingdom*
[3]*CEA, IRFM, F-13108 St-Paul-Lez-Durance, France*

Arc detection is an essential protection system for high power RF systems. It is commonly realised by monitoring the Voltage Standing Wave Ratio (VSWR) in the transmission lines. The JET ILA is a load-tolerant ICRF antenna with a low impedance section, for which the standard VSWR protection is ineffective.

The Scattering-Matrix Arc Detection (SMAD) was proposed and implemented on JET to protect the low-impedance section around the T-junction against arcing. It is based on a consistency check of the RF signals around this section using a table of coefficients obtained from RF modelling.

The paper reviews the SMAD principle, its commissioning on JET and the latest improvements to the system. It shows an example of operation and the time response of the system is analysed. The latest improvements have increased the robustness and reliability of SMAD, making it a choice of arc detection system for critical sections on existing and future RF systems.

Keywords: JET, ICRF, ICRH, ILA, SMAD, Arc Detection

1. Introduction

Arc detection is an essential protection system for high power RF systems as sustained arcing can lead to substantial damage of components in the system. It is commonly realised by monitoring the Voltage Standing Wave Ratio (VSWR) in the transmission lines [1].

The JET ILA is a load-tolerant ICRF antenna composed of 8 short straps grouped in 4 Resonant Double Loops (RDLs) arranged in a 2 toroidal by 2 poloidal array [2]. Each RDL consists of two poloidally adjacent short straps fed through in-vessel matching capacitors from a common vacuum transmission line. Two toroidally adjacent RDLs are fed through a 3dB combiner-splitter (see figure 1).

In this type of antenna, there is a low-impedance section around the T-junction for which the standard VSWR protection is ineffective. The impedance at the T-junction can be adjusted through the matching capacitors and there is an operational advantage in lowering the T-junction impedance as it improves the load resilience of the antenna [2]. It is important to protect this section as damage due to arcing in low voltage areas on RF systems have already been reported (see e.g. [3,4]).

The Scattering-Matrix Arc Detection (SMAD) was proposed and implemented on JET to protect the low-impedance section around the T-junction against arcing. The principle and technical implementation of the JET ILA SMAD has been extensively described in [5]. Its operation in the 2008-9 JET experimental campaigns was reported in [6,7]. Although the principle of the system was proven and the SMAD was used in operation, it was very difficult to operate reliably, and it lacked robustness as it had to be tuned to the specific experimental conditions. Hence, the system needed to be revised and improved.

Section 2 briefly reviews the principle of operation of the SMAD and its implementation on the JET ILA. Section 3 deals with the commissioning of the system and analyses the sensitivity of the system to the signal levels and accuracy. It also highlights the latest improvements to the system since the 2008-9 operation to make it a reliable and robust system. Section 4 reviews the operation of SMAD on plasma. Finally, section 5 reviews the time delays between the arc detection and the actual removal of the power in the lines by the generators.

2. Principle of operation and implementation

The SMAD is a consistency check of the RF signals around a section of interest, here the T-junction, using a table of coefficients obtained from RF modelling.

The signals available for the consistency check around the T-junction on the ILA are the capacitor voltage probes on the antenna-side of the low-impedance section and the Antenna Pressurised Transmission Line (APTL) directional couplers (forward and reflected voltage measurements) on the generator-side of the low-impedance section. These four RF signals are measured in phase and amplitude.

Figure 1 displays the ILA RF circuit for the two upper RDLs (the two lower RDLs have a similar circuit) and highlights the region covered by the SMAD protection system.

** See the author list of "X. Litaudon et al 2017 Nucl. Fusion 57 102001".*
author's email: pierre.dumortier@rma.ac.be

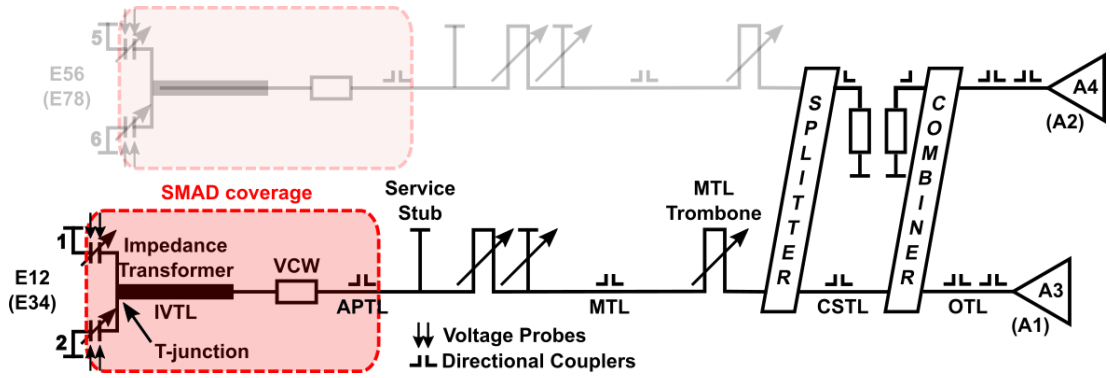

Fig. 1. Schematic of the JET ILA circuit (upper half; similar circuit for the bottom half) and region covered by the SMAD protection. IVTL = Inner Vacuum Transmission Line, APTL = Air Pressurised Transmission Line, MTL = Main Transmission Line, CSTL = Combiner-Splitter Transmission Line, OTL = Output Transmission Line, VCW = VaCuum Window,. A1…A4 are the four 2MW generators.

A comprehensive RF model of the low-impedance section enclosed between the voltage probes and the APTL directional couplers allows the determination of the 3x3 scattering matrices $S_{3x3}(f,C_x,C_y)$ in function of the frequency f for the different values of the variable matching capacitors C_x and C_y. The numerical model of the capacitor, with its moving cylinders and alumina ceramic, is the same as the one used for the voltage probe calibration [8].

The SMAD error function ε_{SMAD} is given by:

$$\varepsilon_{SMAD} = \frac{K_1 V_{Cx} + K_2 V_{Cy}}{K_3 V_{F,APTL,xy} + K_4 V_{R,APTL,xy}} - 1 \qquad (1)$$

where x *and* y are the strap numbers ($x, y = 1…8$), V_{Cx} and V_{Cy} are the voltages measured in phase and amplitude by the capacitor voltage probes and $V_{F,APTL,xy}$ and $V_{R,APTL,xy}$ are respectively the forward and reflected voltages measured in phase and amplitude by the APTL directional couplers of the RDL xy (xy=12, 34, 56 or 78).

The complex coefficients $K_{1…4}(f,C_x,C_y)$ are determined by the RF modelling; they also include the calibration of the RF signals (accounting for all components in the measurement circuit: voltage probes, directional couplers, RF cables, splitters, attenuators, electronics) so that the SMAD directly deals with the raw digital signals in bits.

The error, ε_{SMAD}, will be 0 for an ideal case corresponding to the modelling. In practice the differences between the model and the real object as well as the measurement accuracy and noise will limit the precision and $\varepsilon_{SMAD} \neq 0$.

In absence of arcs the SMAD error will remain below a threshold value, typically $|\varepsilon_{SMAD}| < 0.3$. In case of arc in the protected section $|\varepsilon_{SMAD}| >> 0.3$.

The SMAD complex coefficients $K_{1…4}(f,C_x,C_y)$ are updated through interpolation from look-up tables by the control PXI on a slow time scale, every 10ms. The SMAD error is calculated by a Field Programmable Gate Array (FPGA) on a faster time scale, every 2μs.

3. SMAD commissioning

Different commissioning tests were performed before operation to check the integrity of all components of the system. These tests include checks of the capacitor position reading, SMAD hardware integrity, input and output checks, SMAD error signal calculation and triggering tests. They eventually allowed to identify some error in the FPGA programmed logic implementation treating the SMAD error, which affected operation in 2008-9 by requiring frequency-dependent ad-hoc corrections to the SMAD coefficients [6,7]. These ad-hoc corrections were revised on a shot-by-shot basis and iteratively refined using a minimisation procedure.

Correcting for the FPGA implementation issue together with new numerical modelling and improved accuracy of the measurements through the comprehensive (re)-calibration of all signals [9] allowed to get rid of all ad-hoc corrections needed in 2008-9. This led to a reliable and robust operation of the system, without need of any specific ad-hoc corrections.

Another commissioning test consists in determining the minimum input voltage threshold required. Below this threshold the SMAD error becomes too important. Figure 2 displays the result of this type of test for RDL 56. For this test a signal generator and splitters are used to generate four RF signals, substituting for the measurement signals, which are in phase and roughly equal in amplitude (so that $|V_{Cx}| \sim |V_{Cy}| \sim |V_{F,APTL,xy}| \sim |V_{R,APTL,xy}|$). The amplitude of the RF signals is modulated using a sawtooth waveform. All SMAD coefficients $K_{1…4}$ are imposed equal ($K_{1…4} = 0.8 + 0.8j$ in this example) so that the error ε_{SMAD} should be constant ($\varepsilon_{SMAD} \sim 0.1 + 0j$ in the example due to the slight amplitude difference between the signals). A voltage level > 250 *bit* in amplitude is necessary to keep the SMAD error $|\varepsilon_{SMAD}| < 0.1$ (see figure 2 bottom right). Below this level the error on the phase is such that the SMAD error increases. The threshold for the SMAD error is set on the APTL forward voltage directional coupler. In operation a typical threshold value of 300 *bit* is set, corresponding to a forward power of ~50 *kW*.

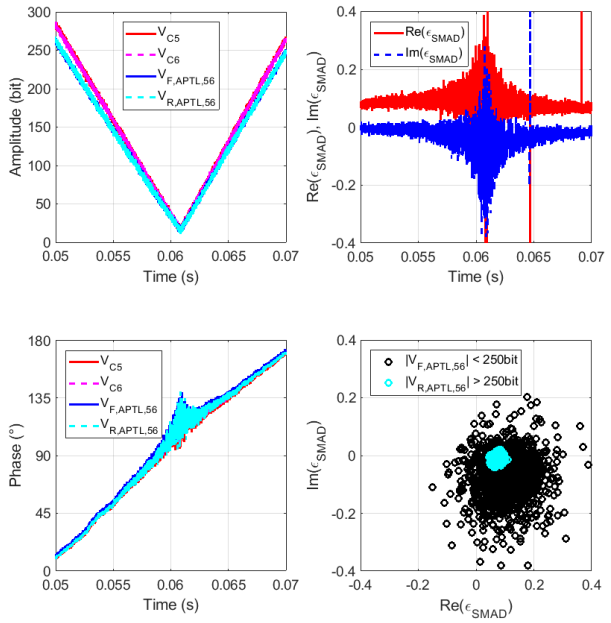

Fig. 2. Amplitude (top left) and phase (bottom left) of the RF signals vs time during a scan in voltage amplitude. Top right: Real and imaginary part vs time of the SMAD error ε_{SMAD}. Bottom right: imaginary part vs real part of the corresponding SMAD error.

Figure 3 displays the result of a test consisting in applying a square modulated signal as input to simulate fast transients for RDL 78. Again, all four signals have roughly the same amplitude and are in phase. The SMAD error remains small ($|\varepsilon_{SMAD}|<<0.1$) and is mainly due to the low values of the signal in the low part of the modulated phase in this case. The spikes observed in the error signal are due to the low levels of the input signals reached during the switch-off of the square wave modulation.

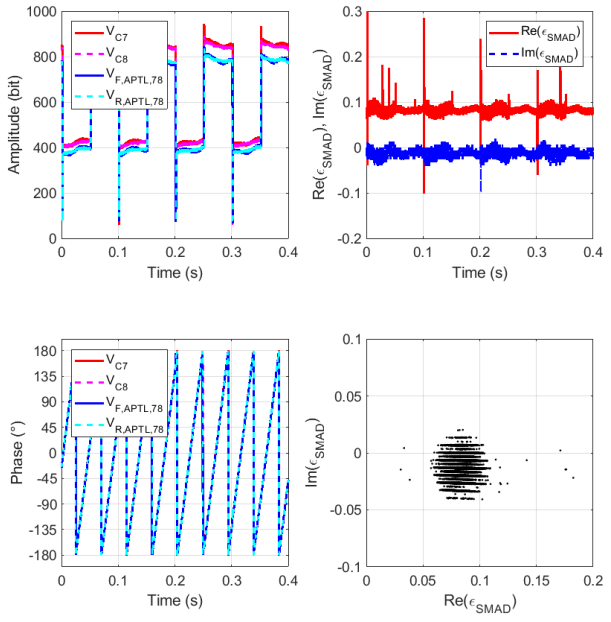

Fig. 3. SMAD error (right) during fast transients simulated by a square wave modulation of the input voltage signals (left).

This test is important to check the insensitivity of the SMAD to fast transients such as Edge Localised Modes (ELMs): it will not issue any false positive trip triggers during ELMs. It is also useful to check that the electronics processing of the signals is adequate, and in particular that the Amplitude and Phase Demodulator Modules (APDMs) electronic filters have the same bandwidth.

Figure 4 displays an example where one signal is modulated to slowly vary the SMAD error in order to check the SMAD trip function. When $|\varepsilon_{SMAD}|$ exceeds the error limit ($\varepsilon_{SMAD,lim}$ = 0.345 in this case) for a chosen number of consecutive points (n = 3 here; one point every $2\mu s$), a SMAD trip signal is produced. The SMAD trip signal stays latched if the (n+1)th point still exhibits $|\varepsilon_{SMAD}| > \varepsilon_{SMAD,lim}$; otherwise the trip signal is reset to healthy.

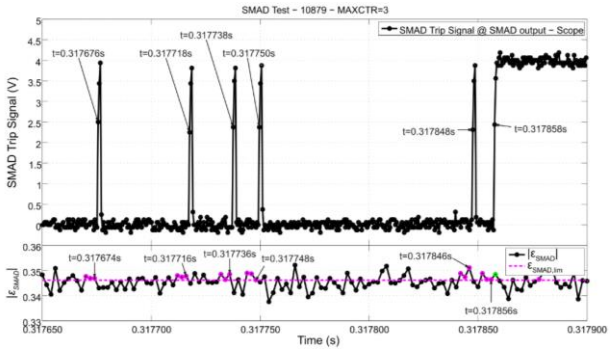

Fig. 4. Scope measurements of the SMAD trip signal (top) and SMAD error signal (bottom). The amplitude of the SMAD error limit, $\varepsilon_{SMAD,lim}$, is set to 0.345 in this example. The SMAD trip is latched if $|\varepsilon_{SMAD}| > \varepsilon_{SMAD,lim}$ for 4 consecutive points.

4. SMAD operation and performance

Numerical simulations of H-mode plasmas show that it is essential to have SMAD active for the detection of low voltage arcs (e.g. T-point arcs) when $\mathrm{Re}(Z_T) < 6\Omega/10\Omega$ while respectively operating half/full ILA antenna array on JET. In these conditions low voltage arcs are indeed not detectable by the traditional Voltage Standing Wave Ratio (VSWR) detection system.

Figure 5 displays an example of operation on an H-mode plasma (RDL 34) at 42.3*MHz*. No arc is occurring in the section under protection. The SMAD error remains below the trip threshold (typically set to $\varepsilon_{SMAD,lim}$ = 0.3 for all frequencies) and all points for which $|V_{F,APTL,34}| < V_{F,APTL,34,thresh}$ = 300 *bit* are within the protection circle.

The SMAD was tested for a wide range of plasma scenarios (in L-mode and H-mode). As discussed in section 3, the table of coefficients is not requiring any ad-hoc correction anymore. It is moreover valid for all tested cases and all operating frequencies; the frequency range was extended in 2015-16 and covers from 29*MHz* to 51*MHz* [10]. The SMAD has been fully re-commissioned and is ready for use as a routine arc protection system during operation in the next experimental campaigns.

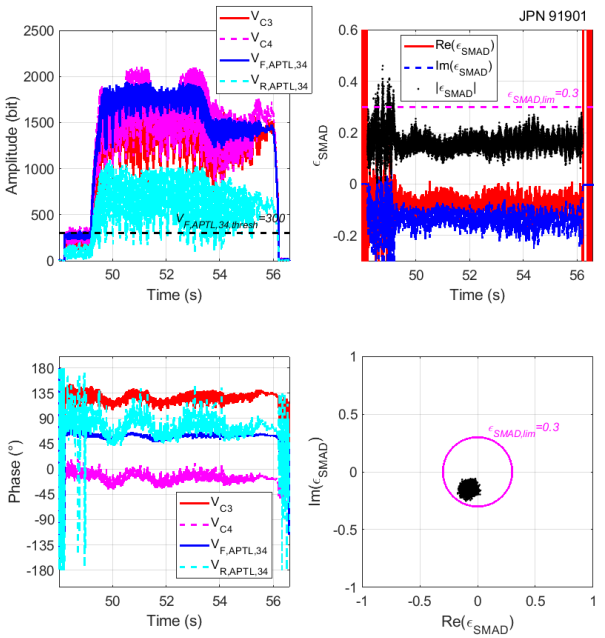

Fig. 5. SMAD signals during healthy operation on H-mode at 42.3MHz for RDL 34. Left: measured signals in amplitude and phase; right: SMAD error. Threshold is set to $V_{F,APTL,34,thresh}$ = 300 *bit* and protection circle is set to $\varepsilon_{SMAD,lim}$ = 0.3.

5. Arc detection time response

The SMAD trip is typically set to latch after 4 consecutive points where $|\varepsilon_{SMAD}| > \varepsilon_{SMAD,lim}$, which corresponds to 8$\mu s$. Scope measurements displayed on figure 6 show the time response at different levels in the chain for a commissioning pulse in test load. The power is removed from the Output Transmission Line (OTL) of the generator after ~25μs, which is within the general protection specifications for the JET ICRF system.

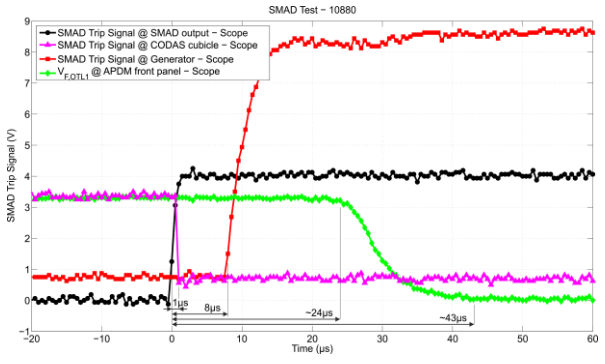

Fig. 6. SMAD response time. Power to the output transmission line is removed ~25μs after the trip signal.

6. Conclusions

The JET ILA SMAD system has been fully re-commissioned. System improvement, new modelling and a comprehensive calibration of the signals allow to operate the SMAD in a robust and reliable manner, without the need of any ad-hoc correction to the coefficients as was the case during the 2008-9 operation.

The SMAD error remains small in the full ILA operation frequency range (extended to 29-51*MHz*) during operation on L-mode and H-mode plasmas, showing that both the RF model of the antenna circuit and the measurements are sufficiently accurate for fast protection. Due to its insensitivity to the RF coupling properties and the fast (2μs) FPGA error calculation, the SMAD is suitable for detecting arcs during ELMs.

The time delay to issue a SMAD trip is typically set to 6-8μs (3-4 FPGA cycles), which is confirmed by scope measurements and fast data signals analysis. The time delay between the trip signal and the removal of the power in the generator output transmission line is measured to be about 25μs, which is within the general protection specifications of the ICRH system on JET.

The SMAD is a mature and robust arc detection system that can be considered to protect critical sections of RF systems in existing (e.g. [11]) and future devices.

Acknowledgments

This work has been carried out within the framework of the EUROfusion Consortium and has received funding from the Euratom research and training programme 2014-2018 under grant agreement No 633053. The views and opinions expressed herein do not necessarily reflect those of the European Commission.

References

[1] R. D'Inca, AIP Conference Proceedings 1406, 5 (2011)

[2] F. Durodié, M.P.S. Nightingale, M.-L. Mayoral, J. Ongena, A. Argouarch, G. BergerBy, et al., Plasma Phys. Control. Fusion 54 (2012) 074012.

[3] K. Vulliez, G. Bosia, S. Brémond, G. Agarici, G. Lombard, L. Million et al., Fusion Engineering and Design 74 (2005) 267-271.

[4] I. Monakhov, V. Bobkov, M. Graham, M.-L. Mayoral, A. Walden and JET EFDA Contributors, AIP Conference Proceedings 933, 151 (2007)

[5] M. Vrancken, A. Argouarch, T. Blackman, P. Dumortier, F. Durodié, M. Evrard, et al., Fusion Engineering and Design 84 (2009) 1953–1960.

[6] M. Vrancken, E. Lerche, T. Blackman, P. Dumortier; F. Durodié, M. Evrard et al., AIP Conference Proceedings 1187 (2009) 237-240.

[7] M. Vrancken, E. Lerche, T. Blackman, F. Durodié, M. Evrard, M. Graham et al., Fusion Engineering and Design 86 (2011) 522–529.

[8] W. Helou, P. Dumortier, F. Durodié, G. Lombard, K. Nicholls and JET contributors, Review of Scientific Instruments 87, 104705 (2016)

[9] P. Dumortier, F. Durodié, W. Helou, I. Monakhov, C. Noble, E. Wooldridge, et al., AIP Conf. Proc. 1689, 070003 (2015).

[10] P. Dumortier, F. Durodié, T. Blackman, M. Graham, W. Helou, E. Lerche, et al., Fusion Engineering and Design 123 (2017) 285–288.

[11] K. Saito, T. Seki, H. Kasahara, R. Seki, S. Kamio, G. Nomura and T. Mutoh, Fusion Engineering and Design 123 (2017) 444–447.